NASA CR-66071

A SURVEY OF SOME BUCKLING PROBLEMS

Bernard Budiansky, Professor
and
John W. Hutchinson, Assistant Professor
Harvard University, Cambridge, Massachusetts

Report SM-8
February 1966

A SURVEY OF SOME BUCKLING PROBLEMS*

REPORT SM-8
February 1966

Bernard Budiansky, Professor
and
John W. Hutchinson, Assistant Professor
Harvard University, Cambridge, Massachusetts

ABSTRACT

Some results recently found in the course of current research on several buckling problems are presented and discussed. These problems are (a) initial post-buckling behavior and imperfection-sensitivity of spherical and cylindrical shells under external pressure (b) initial post-buckling behavior and imperfection-sensitivity of toroidal shells under hydrostatic pressure and tension (c) imperfection-sensitivity of axially compressed cylinders with inside or outside stringers (d) buckling of a model structure having a continuous spectrum of random imperfections (e) dynamic buckling of imperfection-sensitive structures and (f) buckling of spherical caps under concentrated loads.

SYMBOLS

A_s stiffener area

b post-buckling coefficient (see Figure 2)

D shell bending stiffness $\left(\equiv \frac{Et^3}{12(1-\nu^2)}\right)$

E Young's modulus

H spherical cap rise (see Figure 10)

I_s stiffener moment of inertia

K_1, K_3 foundation moduli (see Figure 7)

k parameter in imperfection spectrum (see Figure 8)

L shell length

ℓ $\frac{1}{\pi}$ (buckle length)

ℓ_c critical value of ℓ

N_c classical buckling load per unit length

n circumferential wave number in spherical cap buckling

P load

P_c classical buckling load

P_s static buckling load of imperfect structure

P_D dynamic buckling load

p_c classical buckling pressure

R shell radius (cylinder, sphere, toroidal-segment boundary); correlation function (see Figure 7)

R_x meridional radius of curvature of toroidal segment

s stiffener eccentricity (see Figure 6)

S power spectral density of imperfection (see Figure 7)

W deflection of column

$\overline{W}$ initial deflection of column

Z curvature parameter $\left(\equiv \frac{L^2}{Rt}\sqrt{1-\nu^2}\right)$

δ buckling displacement amplitude

$\overline{\delta}$ initial displacement amplitude

$\overline{\Delta}$ root-mean-square initial displacement

ν Poisson's ratio

INTRODUCTION

This paper contains a brief summary of the results of some recent and current research on several buckling problems. The scope of the survey is arbitrarily limited to investigations with which the writers have been directly or indirectly concerned. Discussion will be made only of phenomena and numerical results, with all the details of analysis omitted. Historical reviews of the backgrounds to the various problems are not included, nor is a comprehensive bibliography of pertinent references provided in this survey.

POST-BUCKLING BEHAVIOR AND IMPERFECTION-SENSITIVITY

The notion of imperfection-sensitivity and its relation to the post-buckling behavior of perfect structures will play an essential role in the problems to be surveyed. The solid curves in Figure 1, based on the studies of Koiter[1,2], illustrate several kinds of bifurcations in the variation of load with buckling displacement that are encountered when buckling of a perfect structure is analyzed as a linear eigenvalue problem. In each case the abscissa is supposed to be a measure of the amplitude of a unique buckling mode corresponding to the buckling load associated with the lowest eigenvalue. The first two sketches illustrate symmetrical bifurcations, for which the initial post-buckling behavior is independent of the sign of the buckling displacement. Only symmetrical bifurcations occur in all of the problems of this paper but asymmetrical bifurcations illustrated in the last sketch are also theoretically possible. The dotted curves show how the applied load varies with displacement when the structure contains an initial deflection in the shape of the buckling mode. If, as shown in the first sketch, the load on the perfect structure drops after buckling, then the load on the imperfect structure attains a local maximum which is lower than the classical buckling load of the perfect structure. Under dead loading this local maximum would be associated with a sudden, possibly catastrophic, increase in displacement which, in a test, would be characterized as buckling. If, as in the case illustrated by the second sketch, the load on the perfect structure

* This work was supported in part by the National Aeronautics and Space Administration under Grant NsG-559, and by the Division of Engineering and Applied Physics, Harvard University.

To be presented at the AIAA/ASME Seventh Structures and Materials Conference, Cocoa Beach, Florida, April 18-20, 1966.

increases after buckling, the corresponding imperfect structure would exhibit a much milder growth of displacement as the load reaches and exceeds the classical buckling load. Finally, if the perfect structure has an asymmetric buckling bifurcation, snap buckling of the imperfect structure would be expected for one sign of the initial imperfection and mild behavior for the opposite sign. Because the buckling strengths of structures characterized by the behaviors shown in the first and the last of the sketches in Figure 1 are influenced by initial imperfections, in some cases markedly so, such structures will be called imperfection-sensitive.

The extent to which imperfections can affect the buckling strengths of imperfection-sensitive shell structures is shown in Figure 2. Suppose that the symmetrical post-buckling load displacement relation is given by the equation

$$\frac{P}{P_C} = 1 + b\left(\frac{\delta}{t}\right)^2 \qquad (1)$$

where P_C is the classical buckling load, δ is the amplitude of the buckling displacement, say normal to the shell, and t is the shell thickness. The coefficient b is then a measure of the rapidity with which the load rises or drops after buckling. Imperfection-sensitive structures would, of course, be characterized by negative values of b. Let P_S be the buckling load of the imperfect structure when it contains an initial imperfection, of amplitude $\bar{\delta}$, in the shape of the buckling mode. Then the solid curves on the right of Figure 2 show how the ratio P_S/P_C varies with the value of $\bar{\delta}/t$. As originally shown by Koiter these curves are governed by the equation

$$\left(1 - \frac{P_S}{P_C}\right)^{3/2} = \frac{3\sqrt{3}}{2}\sqrt{-b}\left|\frac{\bar{\delta}}{t}\right|\left(\frac{P_S}{P_C}\right) \qquad (2)$$

and should really be regarded as correct only in an asymptotic sense for sufficiently small values of the initial displacement.

The most notorious imperfection-sensitive shell structure is probably the long thin-walled cylinder under axial compression which, as is well-known, may buckle at values of stress that are small fractions of the classical buckling stress. Unfortunately, this system is not described by the simple sketches on the left of Figure 2 because it has a multiplicity of buckling mode shapes associated with the classical buckling mode. However, a separate analysis due to Koiter gives the lower dotted curve on the right of Figure 2 for the effect of initial axisymmetric imperfections on the buckling strengths of such cylinders. This curve provides a calibration for the significance of the coefficient b in the case of structures that have just one buckling mode associated with a symmetrical bifurcation. Thus, a value of $b = -1$ would presumably imply imperfection-sensitivity about as severe as that of a cylinder under axial compression. Note, however, that values of b between $-.1$ and -1 would evidently also have quite significant implications and even values of b in the neighborhood of $-.01$ could imply buckling loads smaller than the classical ones by amounts that are not entirely negligible.

In passing, mention can be made of a recent study carried out on another structure that has multiple buckling modes associated with its classical buckling load, namely, the spherical shell under uniform external pressure. It has long been suspected that this structure is about as imperfection-sensitive as the cylindrical shell and this has been theoretically verified very recently[3] on the basis of, again, an asymptotic calculation based on Koiter's general theory, exploiting the shallow shell equations appropriate to very thin shells that buckle with very short wave lengths. The variation of P_S/P_C with $\left(\frac{\bar{\delta}}{t}\right)$ found for the imperfect sphere having a certain checkerboard pattern of initial displacements is given by the dotted curve just above, and nearly coincident with, the curve for the cylinder. Attention will now be directed to the results of studies of several configurations having symmetrical buckling bifurcations with just one buckling mode. The point of these studies was to discover whether and to what extent these configurations are imperfection sensitive by calculating the post-buckling coefficient b. These calculations were all guided by the general theory of post-buckling behavior laid down by Koiter. Within the framework of the shell theories used (Donnell or shallow-shell or a hybrid combination of these) the calculations were exact.

SIMPLY SUPPORTED CYLINDERS UNDER HYDROSTATIC LOADING

The upper curve in Figure 3 provides the classical hydrostatic buckling pressure p_C of a cylindrical shell having conventional simple support boundary conditions. The theoretical results for the nondimensional buckling pressure $\frac{p_C R L^2}{\pi^2 D}$ calculated by Batdorf[4] on the basis of Donnell's equations are plotted against the curvature parameter Z introduced by Batdorf. The results are equally applicable to an isolated shell of length L or to a very long shell continuous over rigid frames having a spacing of L which provide no torsional restraint to the cylinder. In each case, however, pre-buckling deformations are neglected. The lower part of the figure displays the new results just found[5] for the post-buckling coefficient b again plotted against Z. As shown, the parameter b is different for the two configurations even though the classical buckling pressure is the same; the isolated cylinder turns out to be substantially more imperfection-sensitive over the low range of Z than the cylinder continuous over frames. It might be mentioned that there have been previous investigations of the post-buckling behavior of cylinders under hydrostatic loading, with results

that could be described as approximate solutions for finite post-buckling deformations. The present results, in contrast, are asymptotically exact solutions for vanishingly small post-buckling deflections. It is felt that this present kind of solution has greater significance and is perhaps more reliable as an index of imperfection-sensitivity.

The results of buckling tests from a variety of sources (as collected by Dow[6]) are displayed in Figure 3 for comparison with the theoretical classical buckling pressures. The extent to which theory and experiment disagree in various ranges of Z is in qualitative agreement with the degrees of imperfection-sensitivity implied by the negative values of b in these ranges.

TOROIDAL SEGMENTS UNDER HYDROSTATIC LOADING

The top part of Figure 4 shows results recently calculated by Stein and McElman[7] for the classical hydrostatic buckling pressures of simply-supported toroidal segments having various curvature ratios R/R_x, where R represents the radius of the boundary circles and R_x is the meridional curvature. The case $R/R_x = 0$ coincides with the cylinder just discussed. The results of recent calculations[8] of the post-buckling coefficient b are displayed in the bottom part of the figure. The most important implication here is that while the classical buckling pressure increases with increasing values of R/R_x so does imperfection-sensitivity. In other words, increasing the meridional curvature of a toroidal shell would not strengthen the shell against buckling as much as one might hope purely on the basis of a classical buckling analysis. Note that as R/R_x approaches 1 from below the spherical geometry is attained, for which post-buckling calculations on the basis of a unique classical buckling mode may no longer be valid, and so the curiously shaped curves for $R/R_x = .9$ and .95 should be discounted. It may be confidently concluded, however, that, for hydrostatic loading, imperfection-sensitivity disappears only for toroidal segments of sufficiently large negative Gaussian curvature.

TOROIDAL SEGMENTS UNDER AXIAL TENSION

For positive values of R/R_x a toroidal segment under axial tension acquires circumferential compressive stresses and is therefore susceptible to buckling. The results of calculations[8] for the classical axial buckling force per unit length N_c are shown as a function of Z in Figure 5, for several values of R/R_x. The post-buckling coefficient b was found to vary as shown in the bottom part of Figure 5; for each value of R/R_x there is imperfection-sensitivity only for Z larger than the critical value for which b goes negative. Several tests have been performed by Yao[9] for the case $R/R_x = 1$, with results shown by the circles. Yao's specimens were clamped, rather than simply supported but his own calculated buckling loads for this case were only a little higher than those given by the curve in Figure 5. Thus, the discrepancies between the test results and theoretically calculated buckling loads are consistent with the imperfection-sensitivity implied by the negative values of b that were found for simply supported toroidal segments in the ranges of Z corresponding to the test specimens.

STIFFENED CYLINDERS UNDER AXIAL COMPRESSION

There has been much interest recently in the exciting rediscovery of van der Neut's early theoretical observation[10], now well confirmed by tests, that outside stringers can be much more effective than inside stringers in stiffening a circular cylinder against buckling under axial compression. It has been suggested occasionally that classical theories of buckling should be reliable for the quantitative prediction of the buckling loads of stiffened cylinders regardless of whether the stiffeners are inside or outside. Recent calculations[11], however, have shown this not to be so and an example is given in Figure 6 for a simply supported cylinder. If torsional stiffness of the stringers is neglected, three parameters are needed to characterize the stiffening. These are the area ratio A_s/dt, the bending stiffness ratio EI_s/Dt, and the eccentricity ratio $\sqrt{1-\nu^2}\,\frac{s}{t}$ where s, the distance from the skin center line to the centroid of the stringer, is considered to be positive for outside stiffening and negative for inside stiffening. The values chosen for these nondimensional parameters in the present example correspond to only moderately heavy stiffening and are shown in Figure 6. The curves at the top of Figure 6 give, as a function of Z, the buckling load per unit circumference of the stiffened cylinder divided by the corresponding quantity for the unstiffened cylinder, and were calculated on the basis of "smeared-out" stiffener properties. These results imply the superiority of outside over inside stringers. This conclusion, however, must clearly be tempered by the results for the post-buckling coefficient b which show that the cylinder with outside stiffening is generally much more imperfection-sensitive than the one with inside stiffening. It should be emphasized that the coefficient b in this figure is still defined with respect to buckling displacements normalized by the skin thickness and not by any larger effective thickness of the shell-stringer combination. Consequently, over a substantial range of Z in the vicinity of 100 it appears that the effects of initial imperfections in reducing the strength of cylinders with outside stringers below the theoretically predicted classical buckling loads would be by no means negligible. On the other hand, it is interesting to note that in the range of high Z above 1000 both inside and outside stiffeners induce quite comparable imperfection-sensitivity and so the benefits of outside stiffening would appear to be

quite dependable in this range. In any event, the most important conclusion to be drawn is that without supporting evidence, either experimental or theoretical, it would be quite incorrect to assume that classical buckling theory is adequate for the prediction of the buckling strength of stiffened cylinders under axial compression, especially if the stiffening is on the outside.

STRUCTURES WITH RANDOM IMPERFECTIONS

The kinds of investigations just discussed serve to demonstrate whether or not a given configuration is imperfection-sensitive but indicate only qualitatively the degree of such sensitivity; they can not be used to predict the actual buckling load of a given structure that is imperfection-sensitive. One reason for this deficiency is that the initial imperfection certainly does not have precisely the shape of the classical buckling mode, as assumed in the analyses. On the other hand, it does not seem very sensible to attempt to develop methods of analyses based upon a very detailed knowledge of the imperfection in the structure under consideration. A more useful goal might be to attempt to correlate the buckling strengths of imperfect structures with appropriate statistical descriptions of their initial imperfections. To that end the pilot problem illustrated in Figure 7 has recently been studied[12]. In this problem an infinitely long column rests on a nonlinear "softening" foundation and is supposed to have an initial displacement W that is assumed to be a stationary random function of position along the length of the beam. The perfect structure has a continuous spectrum of buckling loads corresponding to the spectrum of buckle modes $\sin x/\ell$ where ℓ can have any value. The critical buckling load P_C however, occurs for a particular value ℓ_C of this wave-length parameter. It is evident that not only will initial imperfections in the shape of the critical buckling mode influence the actual static buckling load of the imperfect structure so will, to some extent, imperfections having any other shape. It is supposed that the mean-square imperfection Δ^2 is known, as is the correlation function R of the imperfection (considered a function of the nondimensional parameter $\xi = x/\ell_C$). The associated power spectral density $S(\phi)$ is defined conventionally as the Fourier transform of the correlation function. The kinds of results that were found for this problem (by means of approximate techniques that lean heavily on the so-called method of equivalent linearization) are illustrated in Figure 8. Shown in this figure is one choice that was made (arbitrarily) for the correlation function of the imperfection, and the associated power spectral density, both characterized by the single parameter k in addition to the mean-square imperfection Δ^2 . The mean-square imperfection combines with the parameters of the foundation modulus to give the pertinent nondimensional parameter $k_3\Delta^2/k_1$ as a measure of the magnitude of the imperfection, and k serves as a measure of the spectral content of the imperfection. The curves show the calculated values of the ratio of the buckling load of the imperfect structure to that of the perfect structure as a function of these two parameters. It is interesting to note that the buckling loads are relatively insensitive to k over a substantial range. This tends to encourage the hope that quantitative predictions of the buckling strengths of imperfection-sensitive structures may eventually be possible on the basis of the knowledge of a few statistical parameters descriptive of the imperfections.

Noted in Figure 8 is an interesting mathematical difference between these results for a structure having a continuous spectrum of buckling modes and the earlier ones for structures having unique buckling modes. In the one-mode case the difference between the buckling loads of the perfect and imperfect structures is, asymptotically, proportional to $(\bar{\delta})^{2/3}$; in the continuous-spectrum case this difference is proportional to $(\bar{\Delta})^{4/5}$.

DYNAMIC BUCKLING OF IMPERFECTION-SENSITIVE STRUCTURES

The general approach of Koiter has recently been extended by the writers[13,14,15] to handle the buckling of imperfection-sensitive structures under a variety of time-dependent loading conditions. General results intended to serve as approximate guidelines for the analysis and design of such structures have thereby been obtained and just one example of this kind of result is illustrated in Figure 9. Consider step-loading of an imperfection-sensitive structure of the type that, when perfect, bifurcates symmetrically, as illustrated,and consequently has a static buckling load P_S less than P_C if it is imperfect. The results of the dynamic analysis show that the same structure having the same imperfection would have a dynamic buckling load P_D given by the graph in Figure 9. Here the ratio of the dynamic to the actual static buckling load of the imperfect structure is plotted against the ratio P_S/P_C , which, of course, equals 1 for the perfect structure and is smaller the more imperfect is the structure. It is seen that for step-loading the dynamic buckling load is always less than the static buckling load, but even for very imperfect structures is never less than 70% of the static buckling load. The most important and useful implication of this curve is that it provides an estimate of the dynamic buckling load just on the basis of P_S/P_C , and does not require a knowledge of the initial imperfection.

SPHERICAL CAP UNDER CONCENTRATED LOAD

The last buckling problem to be discussed in this survey differs in several respects from all of those previously mentioned. The pre-buckling stress state is not trivial, but requires the solution of a nonlinear problem; the buckling loads themselves have not been previously

determined; and in all likelihood the structure is imperfection-insensitive, although this remains to be established theoretically. The clamped shallow spherical shell shown in Figure 10 is subjected to a load P at the center; the solid curve shows how the value of the load parameter $\frac{P_{cr}R}{2\pi D}$ associated with buckling varies with the conventional geometrical parameter λ. This curve gives the lowest of the loads given by the separate curves associated with buckling in various numbers n of circumferential waves. The case $n = 0$ for axisymmetric buckling has previously been obtained by Mescall[16] and corresponds to a local maximum in the variation of load with axisymmetric displacement. The other curves were found[17] by discovering bifurcations of axisymmetric equilibrium paths into non-axisymmetric branches. The mode shapes associated with the cases $n = 3$, 4, and 5, when combined with an axisymmetric dimple, would correspond to deformed areas that are roughly in the shapes of triangles, squares, and pentagons, respectively. Such deformation shapes have in fact been observed in the past during tests on spherical shells under concentrated loads[18,19]. There does not, however, appear to be precise experimental information concerning a critical value of load at which non-axisymmetric deformations first begin to appear, nor has any snapping behavior been discovered in conjunction with their appearance. Indeed, observation has been made[18] of a steady progression of three, four, and five lobed deflection patterns under increasing load and this correlates with the competition shown in Figure 10 among the modes for $n = 3$, 4, and 5. All of these facts suggest that the bifurcation into non-axisymmetric deformation is associated with increasing values of load and verification of this imperfection-insensitive behavior on theoretical grounds is now in progress. It may be noted that the results for λ large are applicable to a full spherical shell of very small thickness. Thus the full sphere under equal and opposite concentrated loads may be expected to begin to exhibit a transition from axisymmetric to non-axisymmetric deformation, at a value of $\frac{PR}{2\pi D}$ near 11.

REFERENCES

1. Koiter, W. T.: "On the Stability of Elastic Equilibrium" (in Dutch), Thesis, Delft, H. J. Paris, Amsterdam.

2. Koiter, W. T.: "Elastic Stability and Post-Buckling Behavior", in "Non-Linear Problems", edited by Langer, R. E., Univ. of Wisconsin Press.

3. Hutchinson, John W.: "Imperfection-Sensitivity of Externally Pressurized Spherical Shells", Report SM-5, Harvard University, October 1965. To be published in Journal of Applied Mechanics.

4. Batdorf, S. B.: "A Simplified Method of Elastic-Stability Analysis for Thin Cylindrical Shells", NACA Rept. 874, 1947 (formerly in NACA TN 1341).

5. Budiansky, Bernard and John C. Amazigo: "Initial Post-Buckling Behavior of Cylindrical Shells under External Pressure", to be published.

6. Dow, D. A.: "Buckling and Post-Buckling Tests of Ring-Stiffened Cylinders Loaded by Uniform External Pressure", NASA TN D-3111, November 1965.

7. Stein, M. and J. A. McElman: "Buckling of Segments of Toroidal Shells", AIAA J., 3, 1704-10 (1965).

8. Hutchinson, John W.: "Initial Post-Buckling Behavior of Toroidal Shell Segments", Report SM-6, Harvard University, November, 1965.

9. Yao, J. C.: "Buckling of a Truncated Hemisphere under Axial Tension", AIAA J., 1, 2316-20 (1963).

10. van der Neut, A.: "General Instability of Stiffened Cylindrical Shells under Axial Compression", National Luchtraartlaboratorium, 13, Report S 314, 1947.

11. Hutchinson, John W. and John C. Amazigo: "Imperfection-Sensitivity of Eccentrically Stiffened Cylindrical Shells", to be published.

12. Fraser, W. Barrie: "Buckling of a Structure with Random Imperfections", Ph.D. Thesis, Harvard University, 1965.

13. Budiansky, Bernard and John W. Hutchinson: "Dynamic Buckling of Imperfection-Sensitive Structures", Proc. XI Internat. Cong. Appl. Mech., Munich, 1964.

14. Hutchinson, John W. and Bernard Budiansky: "Dynamic Buckling Estimates", to be published in AIAA Journal.

15. Budiansky, Bernard: "Dynamic Buckling of Elastic Structures: Criteria and Estimates", Report SM-7, Harvard University, January 1966 (to be published in Proceedings, International Conference on Dynamic Stability of Structures, Northwestern University, October 18-20, 1965).

16. Mescall, J. F.: "Large Deflections of Spherical Shells under Concentrated Loads", Journal of Applied Mechanics, December, 1965.

17. Fitch, James R.: "Buckling and Post-Buckling Behavior of Spherical Caps under Concentrated Load", Ph.D. Thesis research in progress, Harvard Univ.

18. Penning, F. A. and C. A. Thurston: "The Stability of Shallow Spherical Shells under Concentrated Loads", Martin-Marietta Corp., NASA Contractor Report CR-265, July 1965.

19. Evan-Ivanovski, R. M., H. S. Cheng, and T. C. Loo: "Experimental Investigations on Deformations and Stability of Spherical Shells Subjected to Concentrated Loads at the Apex", Proc. 4th U. S. Nat'l. Cong. Appl. Mech., 1962.

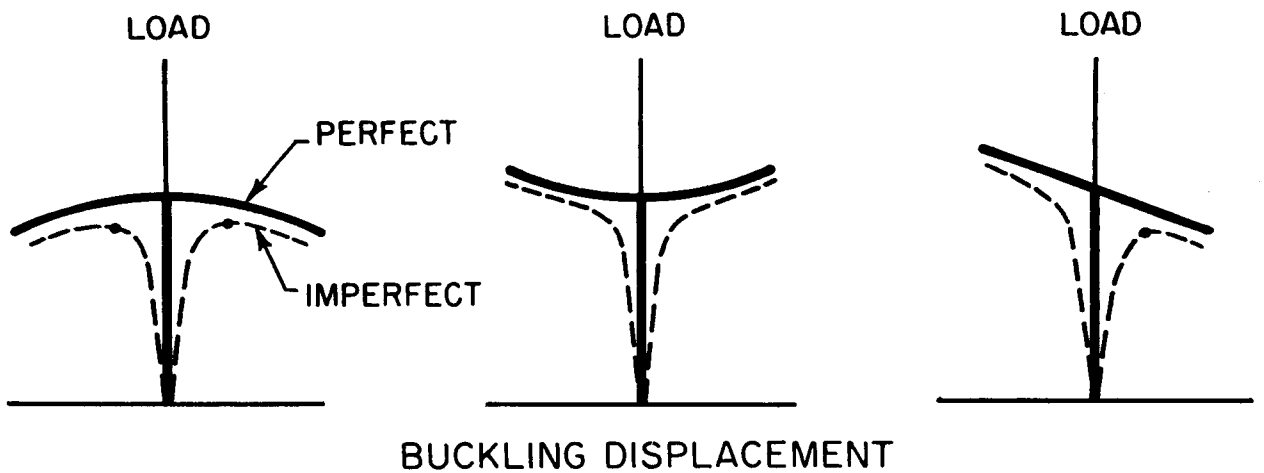

FIG. 1 POST-BUCKLING BEHAVIOR AND IMPERFECTION-SENSITIVITY

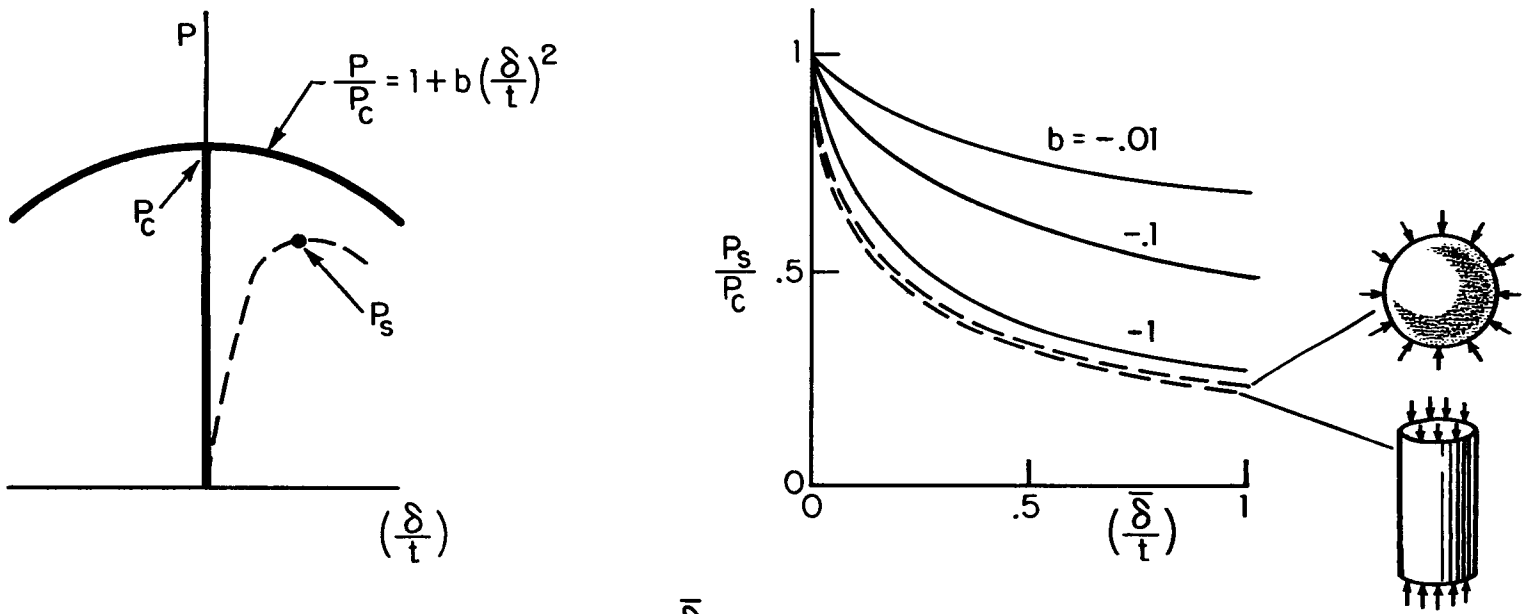

δ = BUCKLING DISPLACEMENT AMPLITUDE

$\bar{\delta}$ = INITIAL DISPLACEMENT AMPLITUDE

t = SHELL THICKNESS

FIG. 2 BUCKLING OF IMPERFECTION-SENSITIVE SHELLS

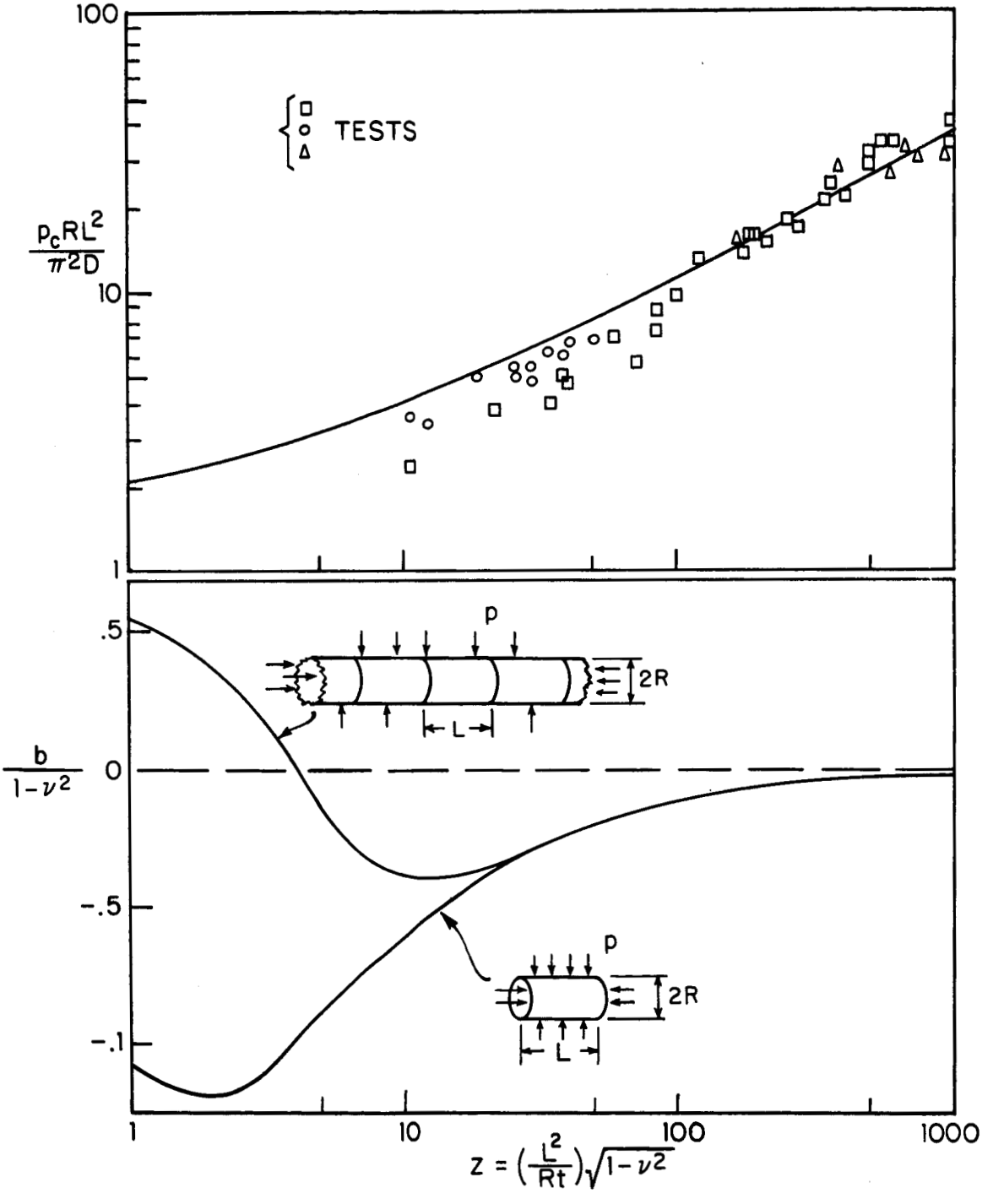

FIG. 3 CLASSICAL BUCKLING AND IMPERFECTION-SENSITIVITY OF SIMPLY-SUPPORTED CYLINDERS UNDER HYDROSTATIC LOADING

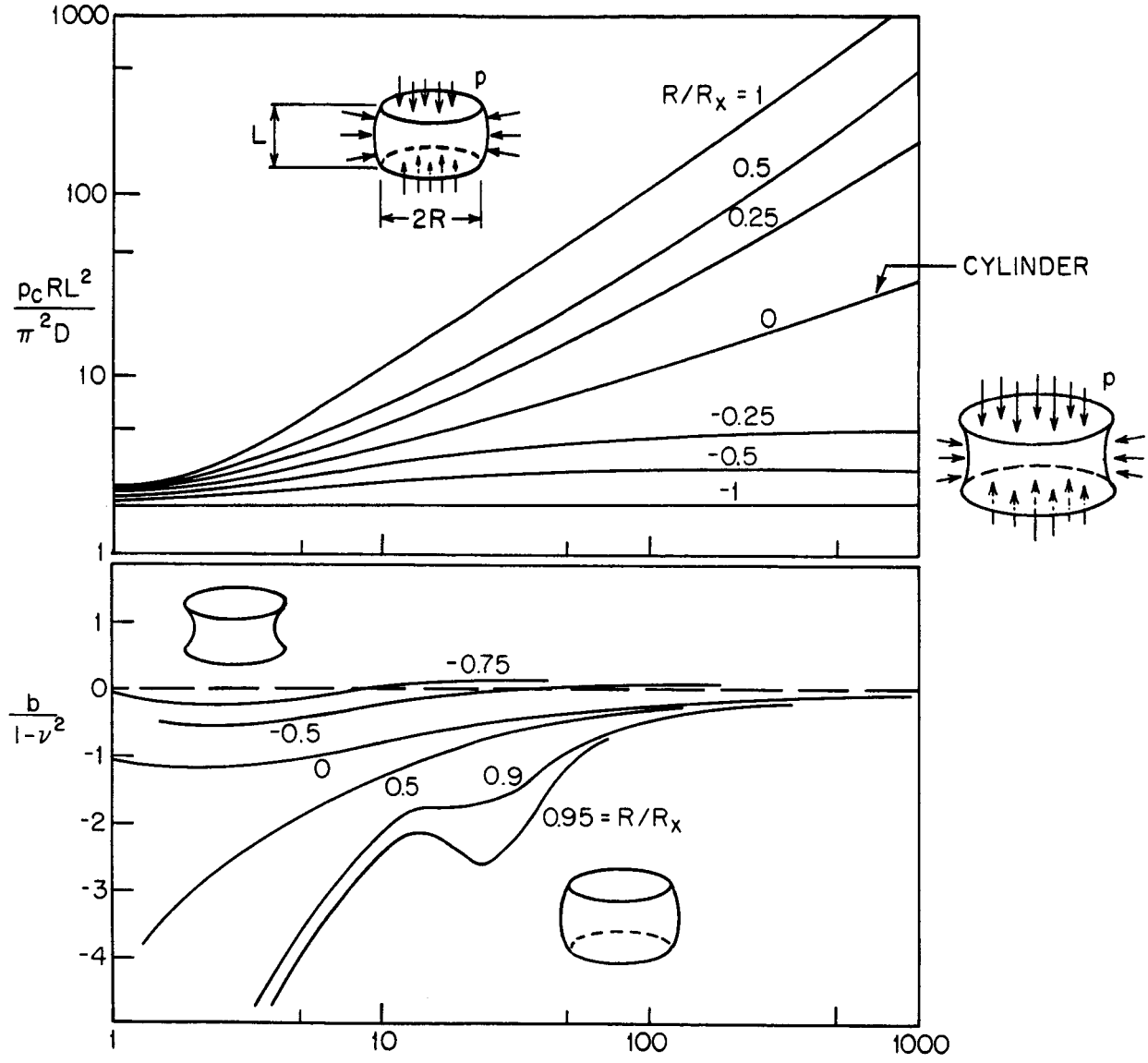

FIG. 4 CLASSICAL BUCKLING AND IMPERFECTION-SENSITIVITY OF SIMPLY-SUPPORTED TOROIDAL SEGMENTS UNDER HYDROSTATIC LOADING

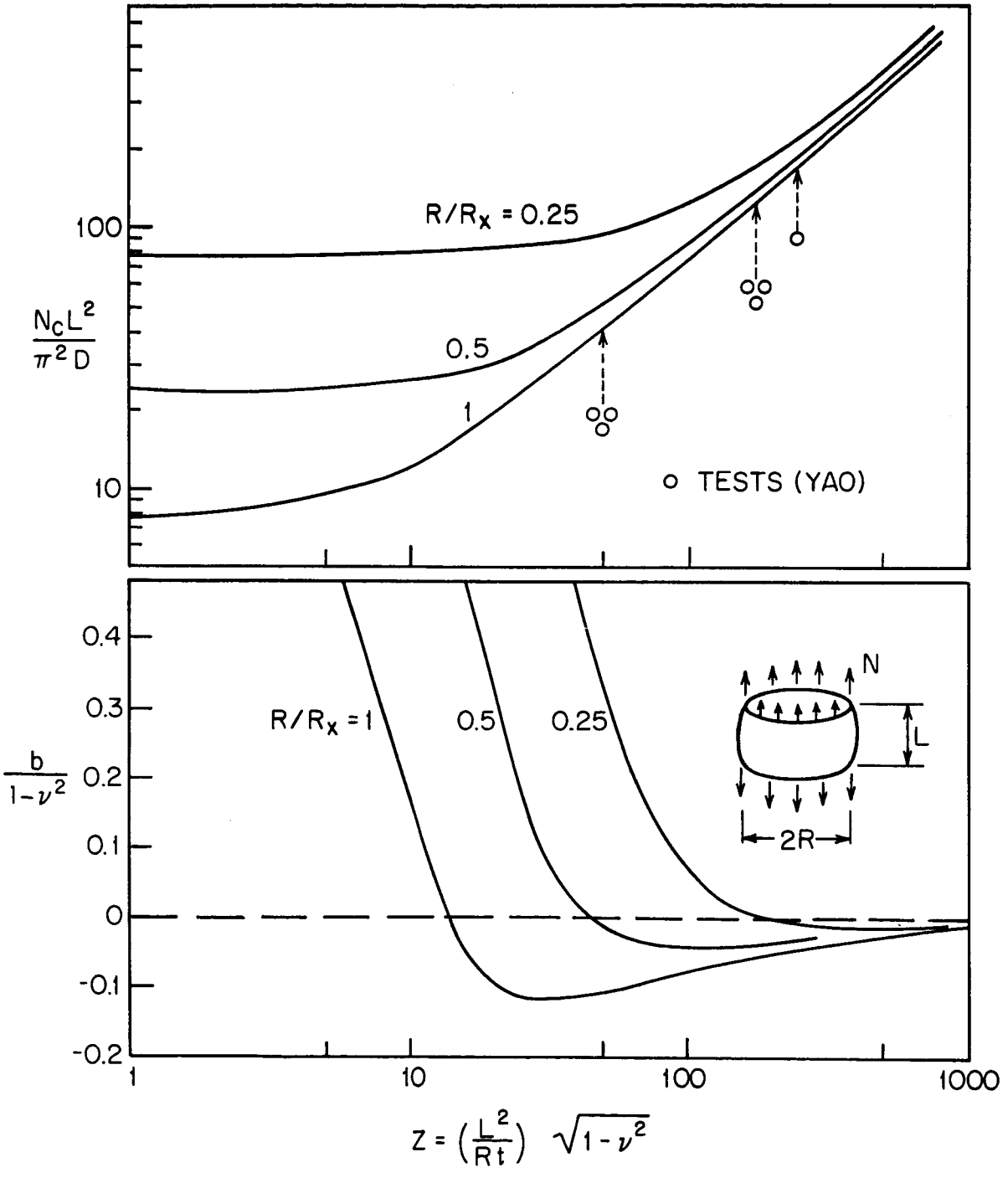

FIG. 5 CLASSICAL BUCKLING AND IMPERFECTION-SENSITIVITY OF SIMPLY-SUPPORTED TOROIDAL SEGMENTS UNDER TENSION

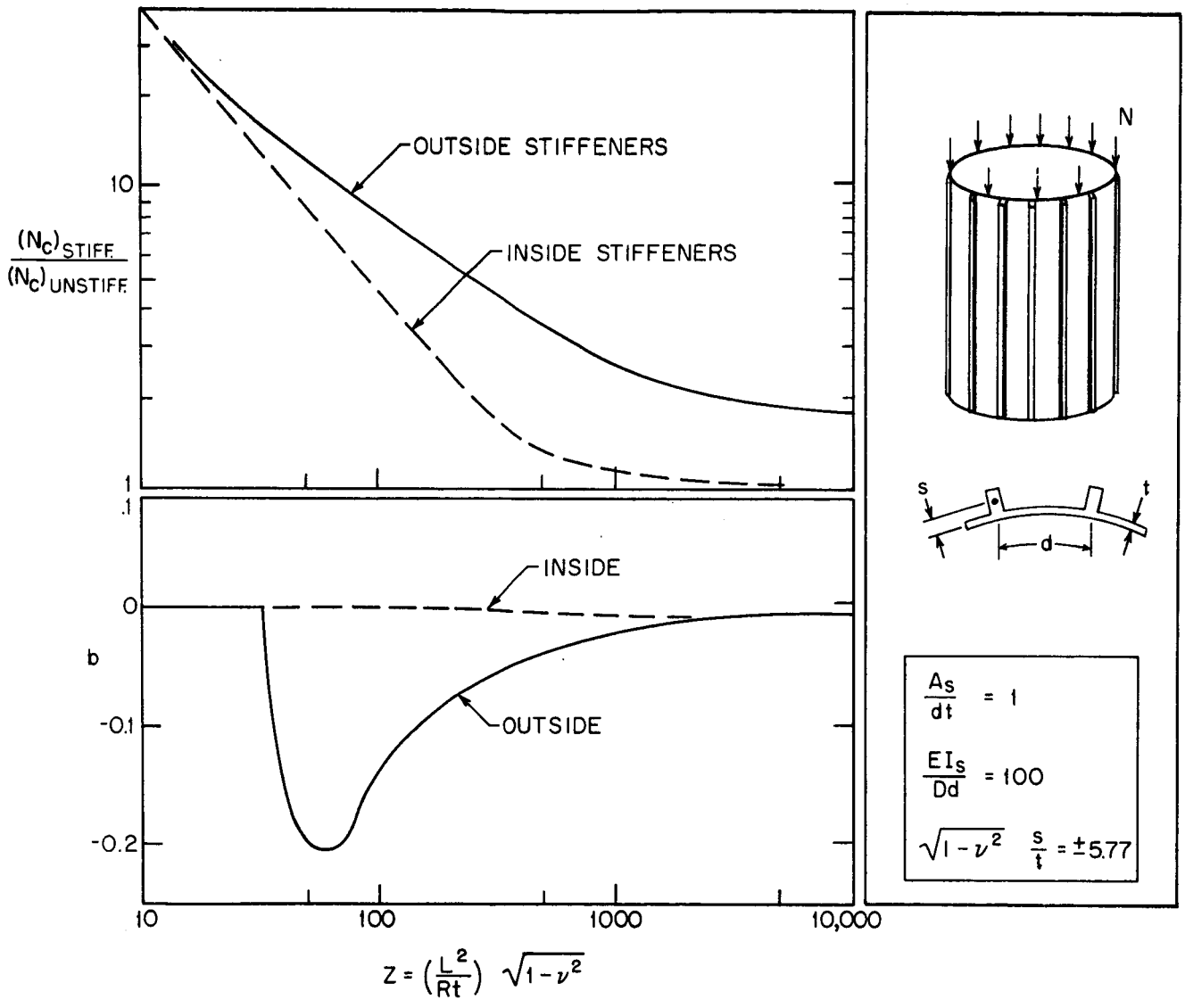

FIG. 6 CLASSICAL BUCKLING AND IMPERFECTION-SENSITIVITY OF SIMPLY-SUPPORTED STIFFENED CYLINDERS UNDER AXIAL COMPRESSION

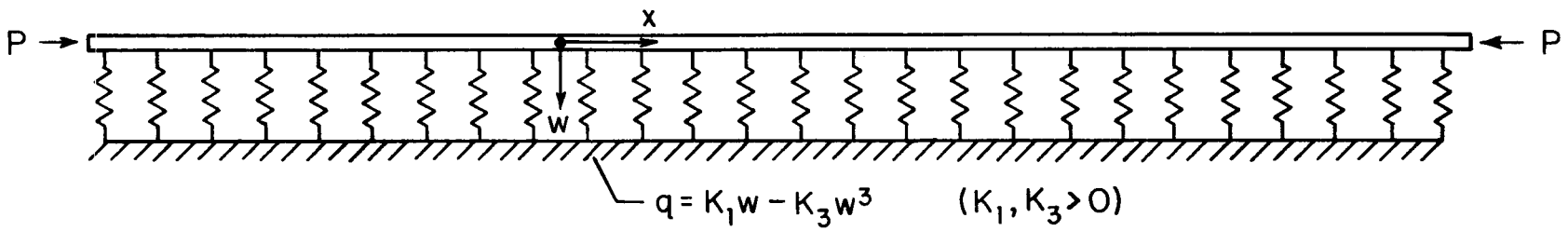

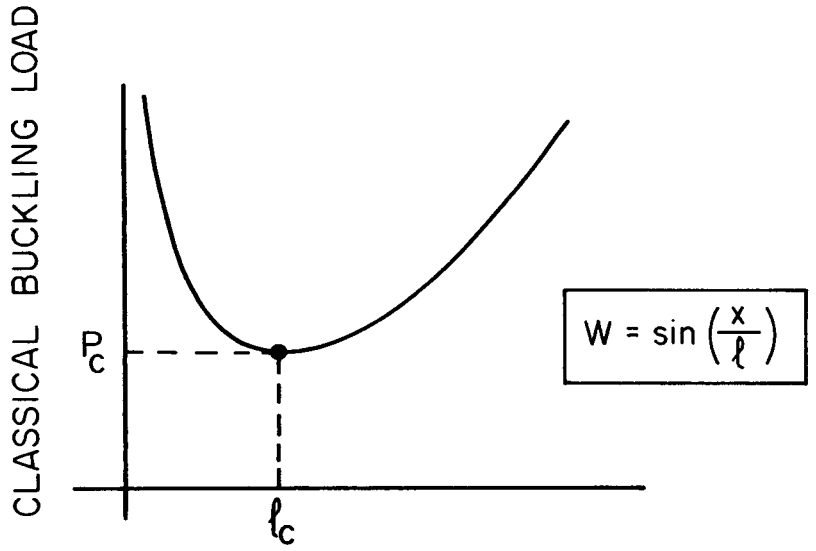

$$\ell = \frac{\text{BUCKLE LENGTH}}{\pi}$$

INITIAL IMPERFECTION: $\overline{W}(\xi) \equiv \overline{W}\left(\frac{x}{\ell_c}\right)$

MEAN-SQUARE IMPERFECTION: $\overline{\Delta}^2$

CORRELATION FUNCTION:

$$R(\eta) = \lim_{\lambda \to \infty} \frac{1}{2\lambda} \int_{-\lambda}^{\lambda} \overline{W}(\xi)\, \overline{W}(\xi + \eta)\, d\xi$$

POWER SPECTRAL DENSITY:

$$S(\phi) = \frac{1}{2\pi} \int_{-\infty}^{\infty} R(\eta) e^{-i\phi\eta}\, d\eta$$

FIG. 7 INFINITELY LONG COLUMN WITH RANDOM INITIAL IMPERFECTIONS ON A NON-LINEAR FOUNDATION

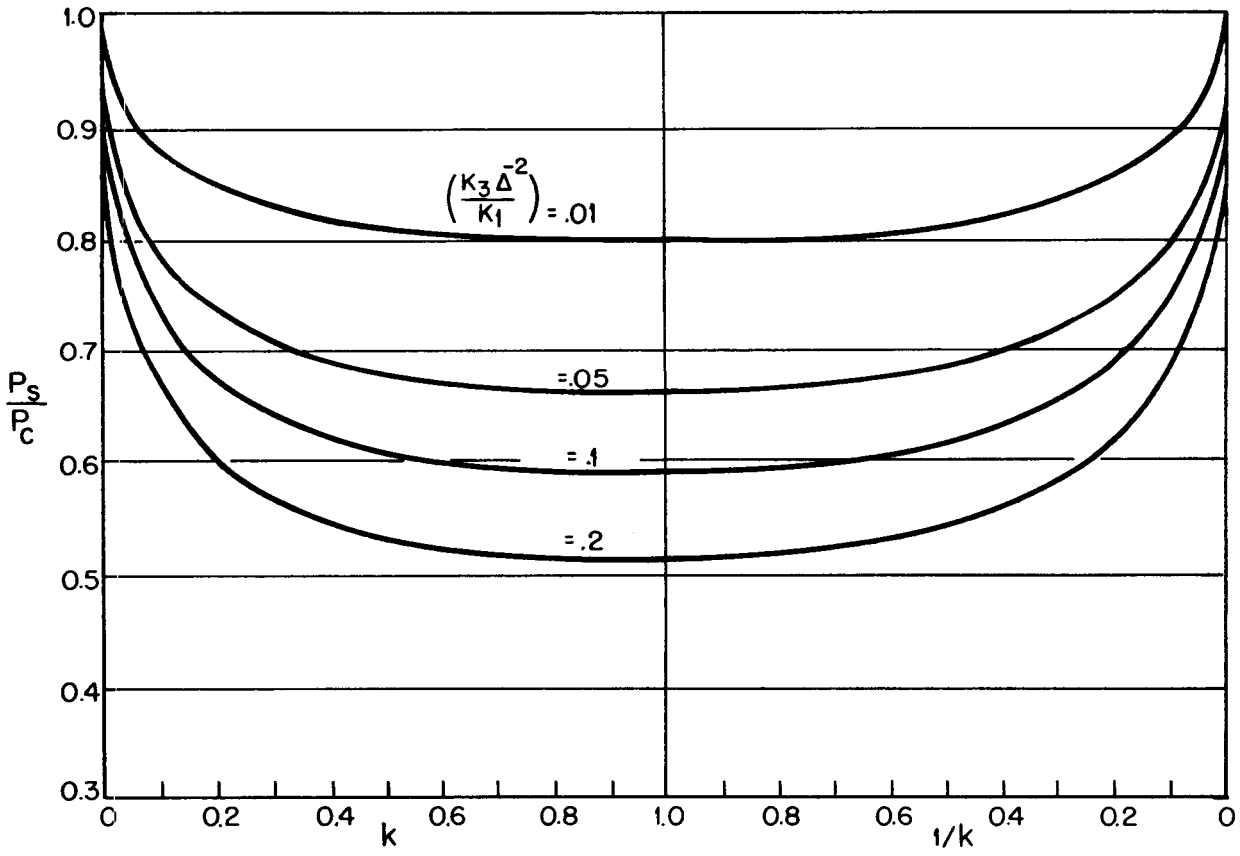

$$\begin{cases} R\left(\frac{x}{\ell_c}\right) = \bar{\Delta}^2 e^{-k\left|\frac{x}{\ell_c}\right|} \\ S(\phi) = \frac{\bar{\Delta}^2}{\pi} \frac{k}{[\phi^2 + k^2]} \end{cases}$$

ONE MODE: $\left(1 - \frac{P_s}{P_c}\right) \sim (\bar{\delta})^{2/3}$

MANY MODES: $\left(1 - \frac{P_s}{P_c}\right) \sim (\bar{\Delta})^{4/5}$

FIG. 8 BUCKLING LOADS OF COLUMN WITH RANDOM IMPERFECTIONS

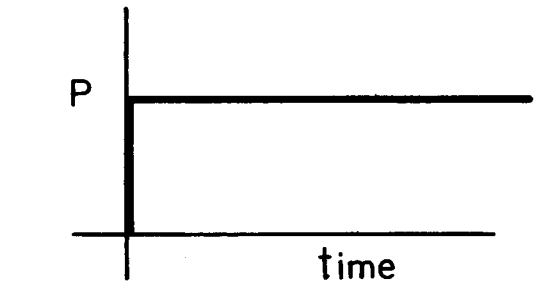

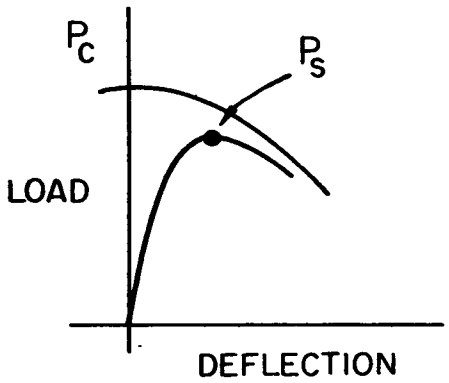

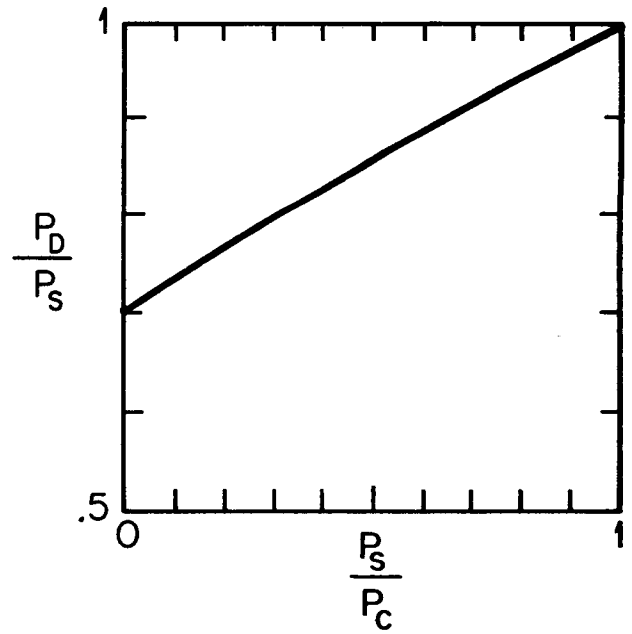

FIG. 9 DYNAMIC BUCKLING, STEP LOADING

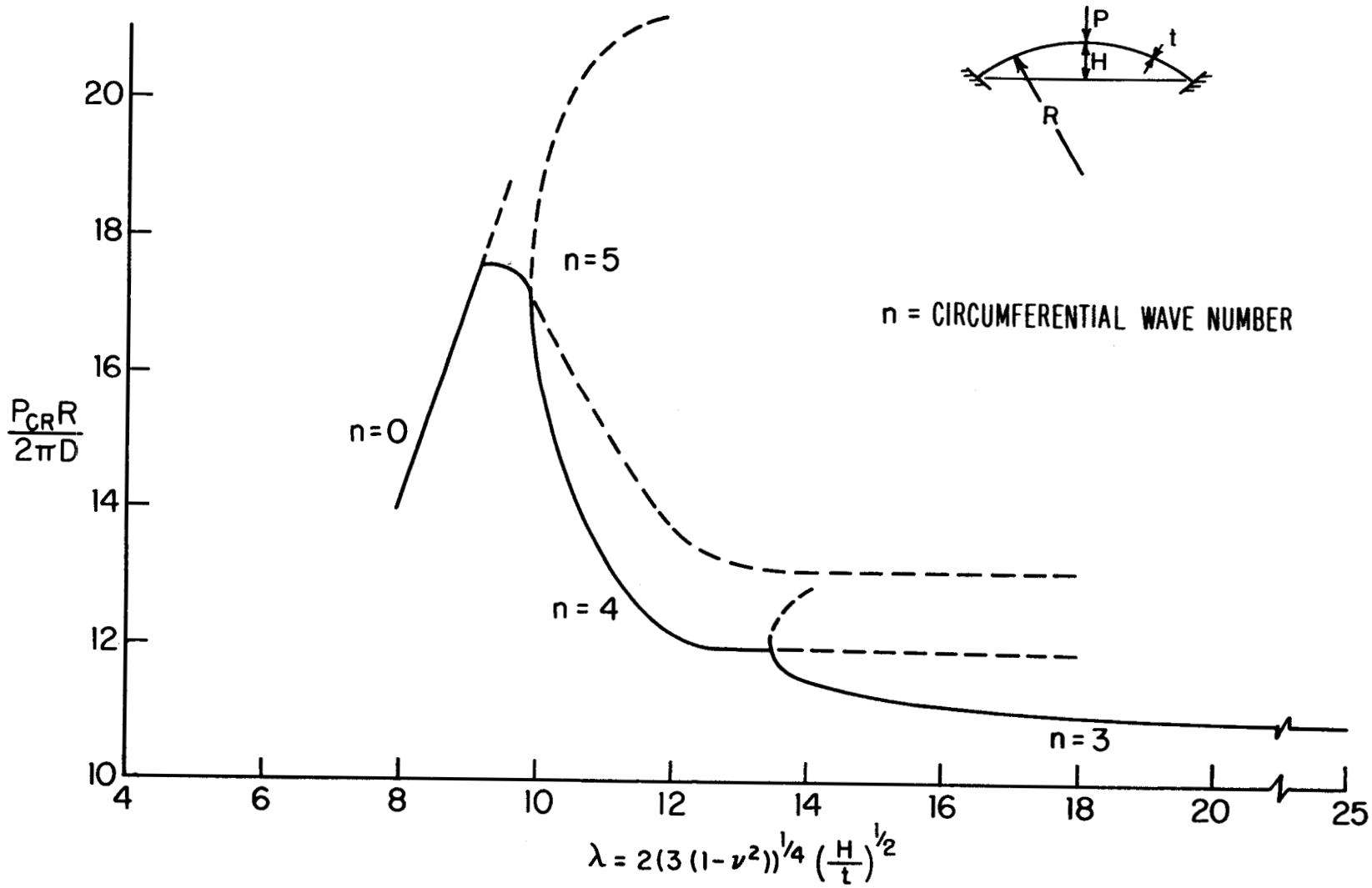

FIG. 10 BUCKLING LOADS FOR CLAMPED SPHERICAL CAP UNDER CONCENTRATED LOAD